Journal of Alloys and Compounds 577 (2013) 79–85

Contents lists available at SciVerse ScienceDirect

Journal of Alloys and Compounds

journal homepage: www.elsevier.com/locate/jalcom

Composition dependent room temperature ferromagnetism and PL intensity of cobalt doped ZnS nanoparticles

B. Poornaprakash [a], D. Amaranatha Reddy [a], G. Murali [a], N. Madhusudhana Rao [b], R.P. Vijayalakshmi [a], B.K. Reddy [a,*]

[a] Department of Physics, S.V. University, Tirupati 517 502, India
[b] School of Advanced Sciences, VIT University, Vellore 632 014, India

ARTICLE INFO

Article history:
Received 30 January 2013
Received in revised form 15 April 2013
Accepted 16 April 2013
Available online 25 April 2013

Keywords:
ZnS:Co
Room temperature ferromagnetism
PL

ABSTRACT

ZnS:Co (0, 1, 2, 3 and 5 at.%) nanoparticles were synthesized by refluxing technique at 80 °C, with PVP as stabilizer. The effect of cobalt doping on the structural, optical and magnetic properties is investigated. EDAX spectra confirmed the presence of Zn, Co and S in the samples. X-ray diffraction patterns showed a single phase that of zincblende and Transmission Electron Microscopy (TEM) indicated that the particles were a few nm (<10 nm) in size. Diffuse Reflectance Spectroscopy (DRS) showed a slight increase in the band gap on doping which further attested the incorporation of Co^{2+} into ZnS nanoparticles as a substituent. Photoluminescence (PL) spectra showed enhanced luminescence intensity with increasing Co concentration. Room temperature magnetization studies revealed that all the Co doped ZnS nanoparticles exhibited ferromagnetic signal which became stronger with increasing Co content. Thus the present studies show that Co doped ZnS nanoparticles may find applications in photoluminescent and spintronic devices.

1. Introduction

Nanometer scale semiconductor crystallites, also referred to as nanoparticles or quantum dots, have been extensively studied to explore their unique properties and potential applications. One key feature that made these materials unique is the possibility of tailoring their electronic properties by doping and through quantum confinement of carriers [1]. In particular diluted magnetic semiconductors (DMSs) have attracted much attention because of their novel applications, due to both charge and spin degrees of freedom of carriers, in spintronic devices such as spin light emitting diodes, spin field effect transistor, and magneto-optical switches [2–4]. In order to make these applications practically viable room temperature ferromagnetic DMS materials are required. Recently, II–VI based DMS nanoparticles have been the focus of numerous research investigations due to their promising applications in laser devices, nonlinear optical devices, electroluminescent, photoluminescent and quantum devices [5,6]. Among all the II–VI semiconductors, ZnS is a nontoxic semiconductor with a wide band gap of 3.68 eV (bulk) [7–9] forms a good host for most of the transition and rare earth metal ion dopants and gives rise to remarkable optical and magnetic properties [10–13]. Doped ZnS nanocrystals have attracted more attention, ever since Bhargava et al. [14] reported for the first time that Mn^{2+} doped ZnS nanosemiconductor could yield both high luminescence efficiency and life time shortening at the same time. The results suggested that the doped semiconductor nanocrystals form a new class of luminescent materials, with a wide range of applications in displays, lighting and sensors [15]. Different workers have reported the optical and magnetic properties of various transition metal doped ZnS nanocrystals [11–18]. Divalent cobalt ion Co^{2+}, with an ionic radius of 0.058 nm [19], which is close to that of divalent Zn^{2+} ion (0.06 nm), can be incorporated in ZnS nanoparticles up to 15–20 at.% [17] by substituting at Zn site without destroying the structure. Also it is a good magnetic ion with a high magnetic moment. Hence, this makes Co doped nanocrystalline ZnS an ideal platform for investigating the optical and magnetic properties. Earlier investigators have reported luminescent and magnetic properties of Co doped ZnO nanoparticles with different results like luminescence enhancement or quenching and presence or absence of ferromagnetism [20,21]. However, reports [17,18,22–25] on Co doped ZnS nanoparticles are still limited and in fact to the best of our knowledge, there is only one report [17] on the magnetic properties of cobalt doped ZnS nanoparticles. In view of these factors and also since room temperature ferromagnetism is reported in Co doped

* Corresponding author. Tel.: +91 9440324223.
E-mail address: Yoursborrak@gmail.com (B.K. Reddy).

0925-8388
http://dx.doi.org/10.1016/j.jallcom.2013.04.106

ZnO [21] which is similar to ZnS, an attempt has been made to synthesize and characterize Co doped ZnS nanoparticles in the present study. II–VI semiconductor nanoparticles are highly unstable, and in the absence of trapping media or some other form of encapsulation, they agglomerate or coalesce easily. To overcome this, bonding of capping agent to nanoparticles is necessary to inhibit formation of larger particles and to improve the surface states that effectively influence the optoelectronic properties of the nanoparticles. Manzoor et al. [26] reported that PVP capped ZnS nanoparticles showed enhanced luminescence properties compared to other capping agents. Hence, PVP has been chosen as a stabilizer in the present investigation.

In this paper, the effect of Co doping on the structural, optical and magnetic properties of PVP capped ZnS nanoparticles formed by refluxing technique is reported.

2. Experimental

ZnS:Co (0, 1, 2, 3 and 5 at.%) nanoparticles were synthesized by refluxing technique at 80 °C. The reactants were zinc acetate dehydrate, cobalt chloride, sodium sulfide and poly vinyl pyrrolidone (PVP). Methanol and distilled water were used as solvents. All the chemicals were of analytical grade and were used without further purification. In a typical procedure, 0.2 M Zinc acetate and required amount of cobalt chloride were mixed with 50 ml of methanol and stirred for 30 min. Separately prepared 0.2 M sodium sulfide solution was added drop wise to the above mixture. Finally, an appropriate amount of PVP was added to the above solution.

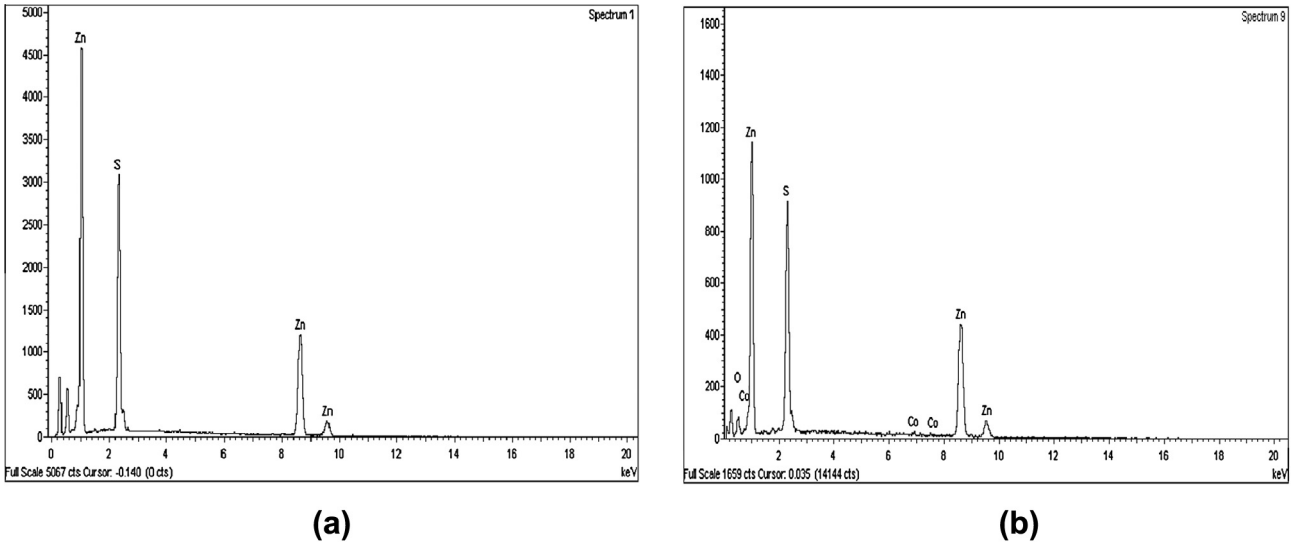

Fig. 1. EDAX spectra of ZnS:Co nanoparticles. (a) Undoped ZnS, (b) 2 at.% Co doped ZnS.

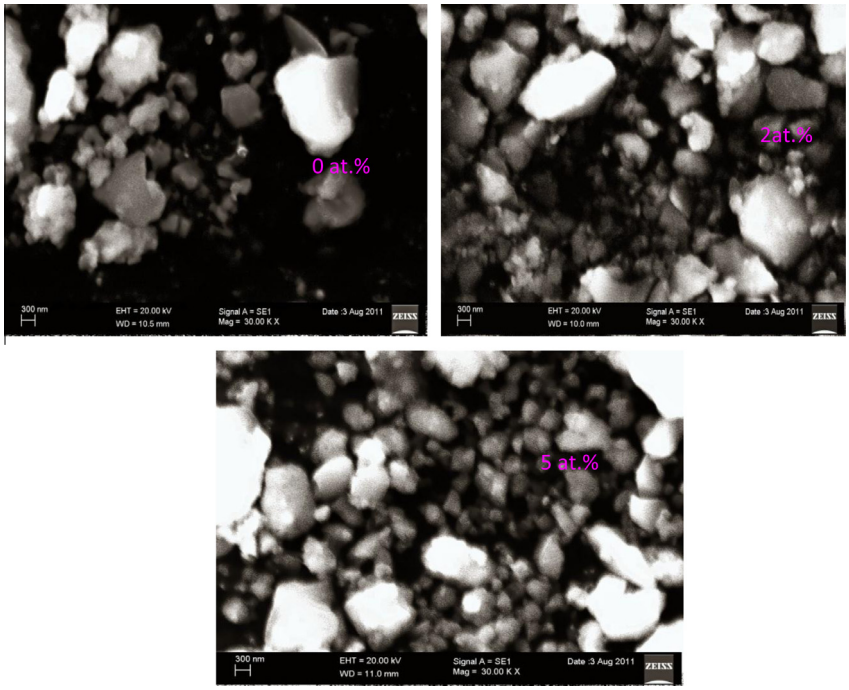

Fig. 2. SEM images of the ZnS:Co (0, 2 and 5 at.%) nanoparticles.

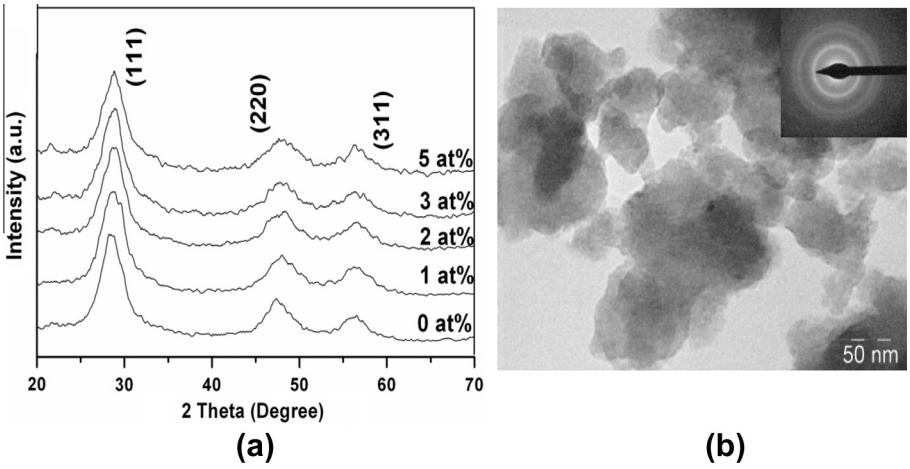

Fig. 3. (a) XRD spectra of ZnS:Co (0, 1, 2, 3 and 5 at.%) nanoparticles. (b) TEM and SAED (inset) image of the ZnS:Co (2 at.%) nanoparticles.

The mixture was refluxed for 3 h at a temperature of 80 °C. The precipitate, containing ZnS:Co nanoparticles, obtained was filtered and washed with ethanol and water many times to remove the impurities and was dried in an oven at 80 °C for 8 h.

Chemical analysis was carried out using a Scanning Electron Microscope (SEM) model, CARL ZEISS EVO MA15, with an EDAX attachment. The structural studies on ZnS:Co nanoparticles were done using Seifert 3003 TT X-ray diffractometer with Cu Kα radiation with a wavelength of 1.540 Å and the system was operated at 30 keV in a scan range of 20–70° Phillips TECHNAI FE 12 Transmission Electron Microscope (TEM) was used for particle size confirmation. Diffuse reflectance measurements were performed using Jasco V-670 double-beam spectrometer for energy gap determination. Photoluminescence studies were carried out using JOBIN YVON Fluorolog-3 spectrometer with a 450 W Xenon arc lamp as an excitation source. Room temperature magnetization was recorded using a Lakeshore Vibrating Sample Magnetometer, VSM 7410. An X-ray Photon Spectrometer (XPS), Model SPECS GmbH (Phoibos 100 MCD Energy Analyser) with Al Kα radiation (1486.6 eV) with a residual pressure of the order of 2×10^{-8} Pa was used to check the presence of impurity phases in the samples.

3. Results and discussion

3.1. Chemical analysis

Fig. 1 depicts the typical EDAX spectra for undoped and cobalt (2 at.%) doped ZnS samples. The chemical analysis shows the presence of Zn, S and Co signals only, indicating that the nanoparticles are made up of zinc, sulfur and cobalt. Only S and Zn signals have been detected in the undoped ZnS samples, suggesting that the nanoparticles indeed are made up of Zn and S only indicating the high purity of the samples.

3.2. Morphological studies

SEM (Scanning Electron Microscope) is a powerful tool to study the surface morphology. Fig. 2 shows typical SEM micrographs of the ZnS:Co (0, 2 and 5 at.%) nanoparticles. These images show that the size of agglomerations slightly decreases with increasing dopant concentration.

3.3. Structural studies

The phase and crystallite size of the nanoparticles were obtained from the XRD patterns. Fig. 3a shows the XRD patterns of the ZnS:Co (0, 1, 2, 3 and 5 at.%) nanoparticles. All these have three main diffraction peaks corresponding to (111), (220) and (311) planes which match well with the standard cubic ZnS (JCPDS No. 05-0566). The broad XRD peaks are indicative of the nanosize of the particles. Further, the peak positions shift towards higher 2θ values with increasing Co concentration. This clearly implies lattice compression consistent with the smaller ionic radius of Co^{2+} (0.058 nm) compared to that of Zn^{+2} (0.06 nm), confirming the incorporation of the dopant as substituent in the synthesized ZnS

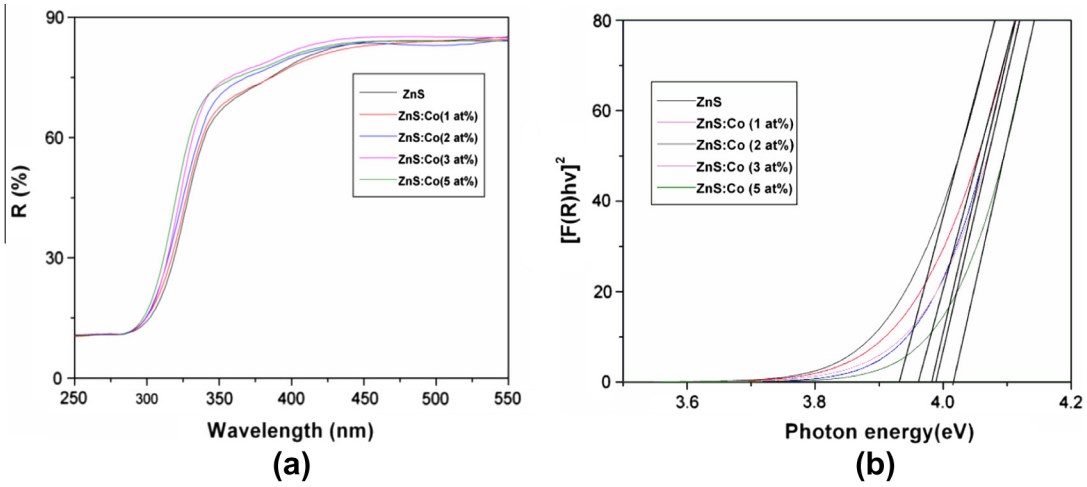

Fig. 4. (a) DRS spectra of ZnS:Co (0, 1, 2, 3 and 5 at.%) nanoparticles and (b) Kubelk–Munk plots and band gap energy estimation for ZnS:Co nanoparticles.

nanoparticles. The average diameter of the particles was estimated using the Scherrer formula,

$$D = 0.89\,\lambda/\beta\,\cos\,\theta,$$

where D is the average size of the particles, β is the full width at half maximum intensity (FWHM) of the diffraction peak, λ is the wave length of X-rays used and θ is the angle of diffraction. The average size of the particles was found to be in the range of 5–8 nm and is found to decrease with increasing Co concentration. Fig. 3b shows typical TEM and SAED (inset) images of ZnS:Co (2 at.%) nanoparticles.

3.4. DRS analysis

The optical properties of the samples were studied by DRS in the UV–Vis region. Fig. 4a shows the DRS spectra recorded at room temperature in the wavelength range of 250–550 nm. From these spectra, it may be observed that the absorption edge of the samples slightly shifted to lower wavelength with increasing Co^{2+} concentration. The band gaps of the samples were estimated from diffuse reflectance spectra by plotting the square of the Kubelka–Munk [27] function F (R) versus energy and extrapolating the linear part of the curve F $(R)^2 = 0$ as shown in Fig. 4b. It is observed that the band gap showed a slight increase with increasing Co^{2+} content. The estimated band gap values of the present samples are in the range of 3.93–4.01 eV which are higher than the bulk band gap value (3.67 eV) of ZnS confirming the nanosize of the particles. Recently Liu et al. [22] reported an increase in band gap with increasing Co content in Co doped ZnS nanoparticles formed by hydrothermal synthesis. Sambasivam et al. [17] also reported similar increase in band gap with increasing Co concentration in $Zn_{1-x}Co_xS$ for $x = 0.1$, 0.2 and 0.3 nanoparticles formed by chemical co precipitation method. Sarkar et al. [23] reported a decrease in band gap in Co doped ZnS nanoparticles compared to undoped ZnS nanoparticles formed by chemical co-precipitation method.

3.5. Photoluminescence studies

The intrinsic and extrinsic defects in semiconductors may be explored by the nondestructive photoluminescence (PL) measurements. This provides information regarding the impurity and defect energy states even when they are present in very low concentrations and therefore is useful to understand defect structures in semiconductors. Fig. 5 shows the room temperature PL spectra of undoped ZnS and ZnS:Co nanoparticles recorded with an excitation wavelength of 344 nm. The emission spectrum of undoped ZnS nanoparticles shows blue emission centered around 442 nm. This originates from the surface defect states such as sulfur vacancies located at the surface of ZnS nanoparticles [28]. Such blue emission was reported by several earlier workers [29–33] also and was attributed to surface defect states of the ZnS nanoparticles. Obviously this emission does not correspond to band edge luminescence of ZnS, because the band gap lies in the range of 3.93–4.01 eV as may be seen from Fig. 4b which correspond to a wave length range of 315–309 nm. A Gaussian fit of the present experimental PL data peaking around 442 nm gave rise to three deconvoluted emission peaks (Fig. 6) peaking around 402 nm, 438 nm and 470 nm. None of these values corresponds to band edge emission. Thus band edge emission is not observed in the present samples. This could be due to the presence of shallow and deep traps below the conduction band due to the surface defects of the nanoparticles.

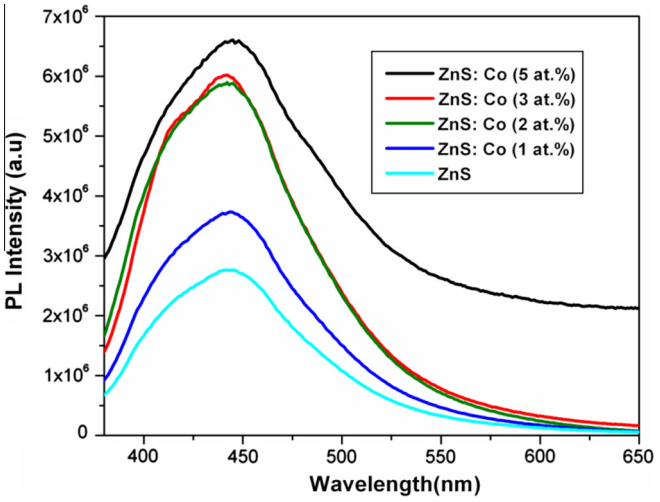

Fig. 5. PL spectra of ZnS:Co (0, 1, 2, 3 and 5 at.%) nanoparticles.

In Co doped samples of the present study the blue emission wavelength does not change with dopant concentration as may be seen from Fig. 5. This indicates that the energy level of defect states/sulfur vacancies relative to the valance band nearly keeps constant. It is also obvious from Fig. 5 that luminescence intensity is appreciably enhanced on doping with Co and also the intensity increases with increasing Co content in the doped samples. This may be correlated with XRD data. It may be observed from Fig. 3 that the full width at half maximum intensity of the XRD peaks increases with increasing dopant concentration indicating that there is a decrease in particle size with increasing cobalt content. A decrease in particle size results in enhanced surface defects leading to an increase in the PL intensity as cobalt content is increased. This indicates that Co^{2+} seems to act as a sensitizing agent [18,23] and thus enhances the radiative recombination processes. Hence, the fluorescence efficiencies of doped samples are higher than those of the undoped samples. Yang et al. [18] reported a five-fold enhancement in the luminescence intensity of Co^{2+} (0.5 at.%) doped ZnS nanoparticles compared to undoped ZnS nanocrystals. Sarkar et al. [23] also observed blue emission with enhanced luminescence intensity in ZnS nanoparticles after doping with Co. Recently Ramasamy et al. [24] studied the photoluminescence properties of Co doped ZnS nanoparticles and concluded that Co concentration of 2 at.% is the optimum doping level to achieve enhanced PL emission. Yang et al. [25] also reported enhanced luminescence intensity in (Co^{2+}, Cu^{2+}) co-doped ZnS nanoparticles compared to undoped ZnS nanoparticles. Recently Sharma et al. [21] observed enhanced fluorescence intensity in Co doped ZnO nanoparticles up to 20 at.% of cobalt doping level due to the increment of oxygen vacancies with Co concentration.

3.6. Magnetic studies

The room temperature (300 K) M–H curves for the undoped and doped samples of ZnS nanoparticles are shown in Fig. 7. These M–H curves depict that the undoped samples are diamagnetic whereas all the doped samples are ferromagnetic in nature. The ferromagnetism is found to increase with increasing Co content. Maximum saturation magnetization (M_s), 0.5 emu/g, was observed for the 5 at.% Co doped ZnS nanoparticles. The weak ferromagnetism of 1 at.% Co doped ZnS samples may be due to the diamagnetic effect of ZnS lattice. The increasing spontaneous magnetic moment observed with increasing Co content indicates that only a fraction of Co ions is magnetically ordered with respect to the applied field. The origin of ferromagnetism in DMS is highly controversial and has been a subject of debate. The observed ferromagnetism of the present samples may be attributed, firstly to the entering of Co in the ZnS lattice as a substituent leading to the carrier induced

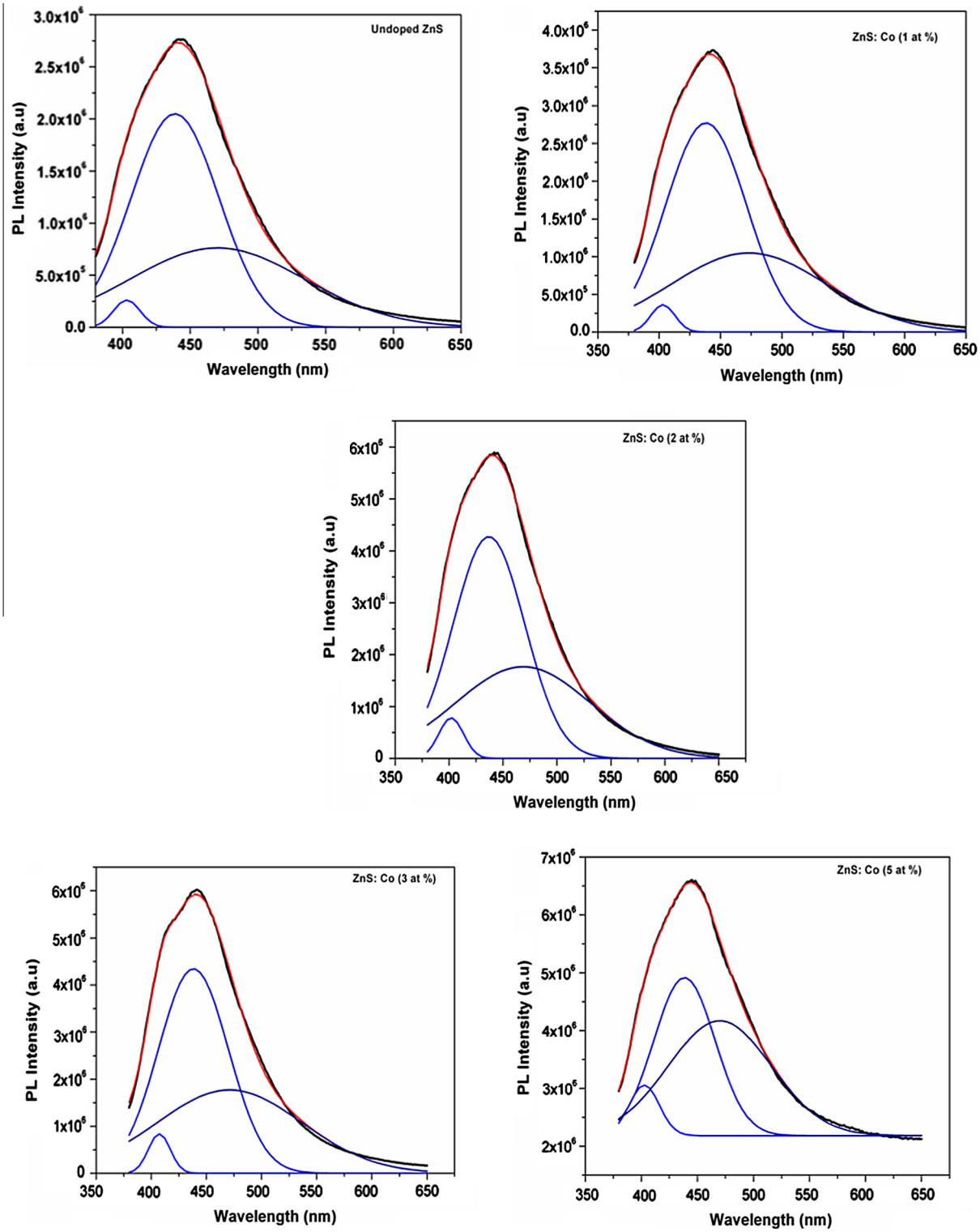

Fig. 6. Gaussian fit (red) of PL data (black) of ZnS:Co (0, 1, 2, 3 and 5 at.%) nanoparticles, blue curves indicate the deconvoluted peaks. (For interpretation of the references to color in this figure legend, the reader is referred to the web version of this article.)

ferromagnetism which is often reported in DMS [34], secondly to inclusion of secondary phases like cobalt oxides and cobalt sulfides and Co clusters which were not detected in the XRD patterns. To resolve this problem XPS (Fig. 8) studies were undertaken and the spectra did not show the presence of either cobalt or cobalt related compounds, although XRD patterns have shown that ZnCoS is formed. It is possible that both XRD and XPS could not detect the cobalt related impurity phases even if they are present. Borse et al. [35] also reported that Ni (5 at.%) and Fe (5 at.%) could not be detected by XPS in their samples. Under these circumstances it is not possible to conclude anything about the origin of ferromagnetism in the present samples. However, the chances of formation of oxides and sulfides of Co are remote since their formation requires elevated temperatures and the present samples are

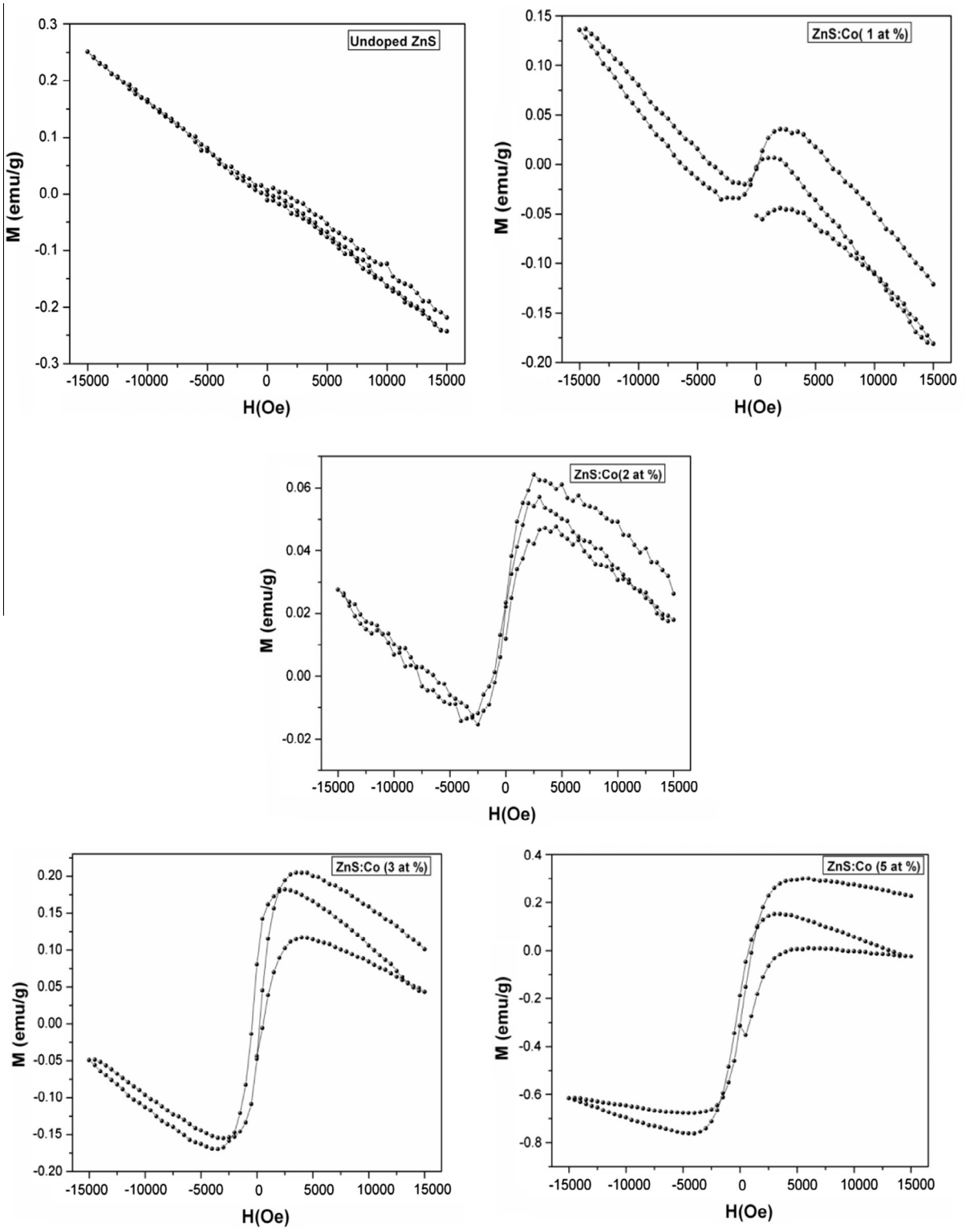

Fig. 7. M–H curves of ZnS:Co (0, 1, 2, 3 and 5 at.%) nanoparticles at room temperature (300 K).

prepared at 80 °C. Thus tentatively the resulting ferromagnetic behavior of the present samples may be attributed to the substitution of Co^{2+} in place of Zn^{2+} in ZnS lattice without changing the structure which implies that this may be carrier induced ferromagnetism. Sambasivam et al. [17] also reported such carrier induced ferromagnetism in Co doped ZnS nanoparticles; $Zn_{1-x}Co_xS$, for $x = 0.1$, 0.2 and 0.3, but they reported a decrease in the magnetization with increasing Co content which was attributed to antiferromagnetic ordering with increasing Co concentration. Perhaps this was because the Co concentrations (10, 20 and 30 at.%) in their samples were much higher, outside the range of the present study, which may lead to strong antiferromagnetic ordering and hence it is not proper to compare with the present trend. Recently Patel et al. [36] also have reported low temperature ferromagnetism in

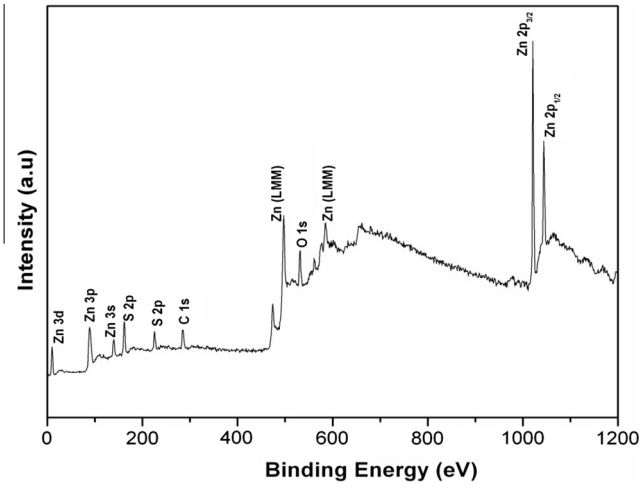

Fig. 8. XPS survey scan of ZnS:Co (5 at.%) nanoparticles.

2.5 at.% Co and room temperature ferromagnetism in 5 at.% cobalt doped ZnS thin films and suggested that the grain boundaries may play a role in bringing about the ferromagnetic order.

4. Conclusions

The structural, optical and magnetic properties are found to be sensitively dependent on the incorporation of Co^{2+} ions at the Zn^{2+} lattice site. The small shift in the XRD peak confirms the entry of Co ions as substituents in the lattice of ZnS nanoparticles. The doping of Co^{2+} ion can tune the band gap and enhance the fluorescence efficiency of the ZnS nanoparticles. The doping of Co^{2+} ion in ZnS nanoparticles showed marked enhancement room temperature ferromagnetism which increased with increasing Co content in the concentration range 1–5 at.%. Homogeneous distribution of substitutional dopant ions in the host lattice is believed to be responsible for the magnetization enhancement. Thus the present study shows that PL intensity and RTFM may be tuned as a function of dopant concentration in ZnS:Co nanoparticles indicating their possible applications in photoluminescent and spintronic devices.

Acknowledgements

The authors are highly grateful to the University Grants Commission, New Delhi, India, for providing the financial support. The authors are thankful to Mr. N. Sivaramakrishnan and Mr. Muthukumaran, SAIF, IIT Madras, Chennai for extending the VSM facility and to Prof. V. Rajagopal Reddy, Semiconductor Physics Research Center, Chonbuk University, Republic of Korea and to Prof. G. Mohan Rao, Indian Institute of Science, Bangalore, India, for doing the XPS studies independently.

References

[1] A.P. Alivisatos, Science 271 (1996) 933–997.
[2] J.M. Kikkawa, D.D. Awschalom, Nature 397 (1999) 139–141.
[3] I. Zutic, J. Fabian, S.D. Sarma, Rev. Mod. Phys. 76 (2004) 323–410.
[4] Y.S. Didosyan, H. Hauser, G.A. Reider, W. Teriser, J. Appl. Phys. 95 (2004) 7339–7341.
[5] N. Kumbhojkar, V.V. Nikesh, A. Kshirsagar, S. Mahamuni, J. Appl. Phys. 88 (2000) 6260–6264.
[6] N. Goswami, P. Sen, J. Nanopart. Res. 9 (2007) 513–517.
[7] S. Wageh, Z.S. Ling, X. Xu-Rong, J. Cryst. Growth 255 (2003) 332–337.
[8] M. Oshikiri, F. Aryasetiawan, Phys. Rev. B 60 (1999) 10754–10757.
[9] A. Chatterjee, A. Priyam, S.C. Bhattacharya, A. Saha, Colloids Surf. A 297 (2007) 258–266.
[10] B.C. Cheng, Z.G. Wang, Adv. Funct. Mater. 15 (2005) 1883–1890.
[11] S.D. Han, K.C. Singh, H.S. Lee, T.Y. Cho, J.P. Hulme, C.H. Han, I.S. Chun, J. Gwak, Mater. Chem. Phys. 112 (2008) 1083–1087.
[12] N. Karar, H. Chander, J. Nanosci. Nanotechnol. 5 (2005) 1498–1502.
[13] D. Amaranatha Reddy, G. Murali, R.P. Vijayalakshmi, B.K. Reddy, Appl. Phys. A 105 (2011) 119–124.
[14] R.N. Bhargava, D. Gallager, X. Hong, A. Nurmikko, Phys. Rev. Lett. 72 (1994) 416–419.
[15] K.E. Waldrip, J.S. Lewis III, Q. Zhai, M.R. Davidson, P.H. Holloway, S.S. Sun, Appl. Phys. Lett. 76 (2000) 1276–1278.
[16] Nie Eryong, Liu Donglai, Zhang Yunsen, Bai Xue, Yi Liang, Jin Yong, Jiao Zhifeng, Sun Xiaosong, Appl. Surf. Sci. 257 (2011) 8762–8766.
[17] S. Sambasivam, D. Paul Joseph, J.G. Lin, C. Venkateswaran, J. Solid State Chem. 182 (2009) 2598–2601.
[18] P. Yang, M. LuE, D. XuE, D. Yuana, C. Songa, G. Zhoub, J. Phys. Chem. Solids 62 (2001) 1181–1184.
[19] R.D. Shannon, Acta Cryst. A 32 (1976) 751–767.
[20] Sekika Yamamoto, J. Appl. Phys. 111 (2012) 094310–094315.
[21] Prashant K. Sharma, Ranu K. Dutta, Avinash C. Pandey, J. Colloid Interface Sci. 345 (2010) 149–153.
[22] Lingyun Liu, Lin Yang, Pu Yunti, Dingquan Xiao, Jianguo Zhu, Mater. Lett. 66 (2012) 121–124.
[23] R. Sarkar, C.S. Tiwary, P. Kumbhakar, A.K. Mitra, Physica B 404 (2009) 3855–3858.
[24] V. Ramasamy, K. Praba, G. Murugadoss, Spectrochim. Acta Part A 96 (2012) 963–971.
[25] Ping Yang, Lu Mengkai, Guangjun Zho, Duo Rong Yuan, Dong Xu, Inorg. Chem. Commun. 4 (2001) 734–737.
[26] K. Manzoor, S.R. Vadera, N. Kumar, T.R.N. Kutty, Solid State Commun. 129 (2004) 469–473.
[27] A. Escobedo Morales, E. Sanchez Mora, U. Pal, Rev. Mex. Defisica S 53 (2007) 18–22.
[28] S. Lee, D. Song, D. Kim, J. Lee, S. Kim, I.Y. Park, Y.D. Choi, Mater. Lett. 58 (2004) 342–346.
[29] N. Karar, F. Singh, B.R. Mehta, J. Appl. Phys. 95 (2004) 656–660.
[30] P.K. Ghosh, Sk. F. Ahmed, S. Jana, K.K. Chattopadhyay, Opt. Mater. 29 (2007) 1584–1590.
[31] W.Q. Peng, G.W. Cong, S.C. Qu, Z.G. Wang, Opt. Mater. 29 (2006) 313–317.
[32] Yu Carley Corrado, Fadekemi Oba Jiang, Mike Kozina, Frank Bridges, Jin Z. Zhang, J. Phys. Chem. A 113 (2009) 3830–3839.
[33] S. Sambasivam, B. Sathyaseelan, D. Raja Reddy, B.K. Reddy, C.K. Jayasankar, Spectrochim. Acta Part A 71 (2008) 1503–11506.
[34] S. Koshihara, A. Oiwa, M. Hirasawa, S. Katsumoto, Y. Iye, C. Urano, H. Takagi, H. Munekata, Phys. Rev. Lett. 78 (1997) 4617–4620.
[35] P.H. Borse, N. Deshmukh, R.F. Shinde, S.K. Date, S.K. Kulakarni, J. Mater. Sci. 34 (1999) 6087–6093.
[36] Shiv P. Patel, J.C. Pivin, A.K. Chawla, Ramesh Chandra, D. Kanjilal, Lokendra Kumar, J. Magn. Magn. Mater. 323 (2011) 2734–2740.